

MODELING OF ECCENTRIC ROTOR DYNAMICS IN AN UNBALANCED MAGNETIC FIELD

*Goroshko A., Zembytska M.
Khmelnyskyi National University, Ukraine*

Abstract. The paper studies the dynamics of a three-phase induction motor with squirrel cage rotor, which has eccentricity of different kinds. For this purpose, a mathematical model of oscillations of a rigid rotor with mass eccentricity, which oscillates on two elastic supports, is established. The model is further extended to take into account the forces of unbalanced magnetic pull, which arise under static and dynamic magnetic eccentricity. A simulation model in Simulink/Simscape Multibody environment is created to solve the obtained nonlinear model. The simulation of induction motor dynamics is carried out and the vibration signals are analyzed in time and frequency domain. Vibrations caused by static magnetic eccentricity occur at twice the electrical frequency. Vibrations caused by dynamic eccentricity take the form of a rotor frequency signal modulated by a low frequency depending on the rotor precession. The model can be used for vibration diagnostics of motor rotor eccentricity.

Keywords: Vibration, squirrel-cage induction motor, rotor eccentricity, UMP

Introduction

Electric machines are increasingly being used in a wide variety of industries due to a number of advantages, such as high efficiency and the ability to be directly connected to the drive's working body. One of the challenges in the design and operation of electric motors is the high level of vibration. Vibration is the main cause of bearing failure and a source of noise. The main cause of motor vibration is an unbalanced rotor [1].

The quality of rotor operation directly determines the performance of the motor. Rotor imbalance can occur both due to rotor mass eccentricity, when the center of inertia does not lie on the rotor axis of rotation, and due to unbalanced magnetic pull (UMP). Since in most cases the motor rotor can be considered rigid, the problem of rotor mass eccentricity is usually successfully solved by balancing. More difficult to solve is the problem of unbalance caused by magnetic forces, in particular UMP. Under ideal conditions, the air gap between the stator and rotor is uniform and symmetrical. Under this condition, the resulting radial magnetic attraction force around the rotor circumference is zero [2]. However, in practice, the air gap is not uniform in the circumferential direction for various reasons of manufacturing, assembly, and operation. The resulting radial magnetic attraction force of the rotor is no longer zero, and this magnetic attraction force is called the unbalanced magnetic force [1]. Magnetic eccentricity and UMP causes additional radial load on the bearing, which, firstly, reduces its service life, and secondly, further increases UMP.

A distinction is made between static and dynamic eccentricity. Static eccentricity occurs due to the eccentric position of the rotor in the stator bore, so the non-uniform configuration of the air gap does not change in time when the rotor rotates. [3]. In dynamic eccentricity, which occurs due to the eccentric position of the rotor relative to the shaft axis, the configuration of the air gap changes during rotor rotation, which is due to the rotation of the rotor axis relative to the stator axis. Given the small size of the air gap of induction motors, even a small rotor eccentricity, violating the symmetry of the machine design, significantly deteriorates its performance.

Related works

Many papers have been devoted to the problem of induction motor vibrations, and, in particular, to the study of UMP. Paper [3] proposes proactive damping of vibrations caused by unbalanced voltage. To do this, the authors used MATLAB/Simulink software to implement the designed active power filter to dampen the oscillations of an induction motor. The authors

of [4] studied the UMP by the finite element method and obtained the dependences of vibration characteristics at static, dynamic, and mixed eccentricities. Paper [5] additionally investigated the force and stiffness of the UMP and showed that dynamic eccentricity has a more dangerous effect on vibrations, reducing the rigidity of the system. Paper [6] presents a multi-body model of a powerful induction motor on a compliant foundation. By analyzing the vibrations for different slip values, the effect of electromagnetic field damping is shown. In [7], this paper addresses the use of pole-specific search windings in a wound rotor induction motor and proposes their use in condition monitoring systems. The authors of [8] conducted a thorough study of torque harmonics and current harmonics of the stator of an induction motor. The obtained results help to identify the origin of these harmonics as a result of the interaction of the stator current and magnetic induction from the rotor in the air gap.

Despite the existence of studies on the subject of induction motor vibrations under the influence of UMP, the mechanism of UMP occurrence, the interaction of mass and magnetic unbalance forces, and possible solutions to the problem require additional research. For this purpose, this paper proposes a simulation model of a rotor with mass eccentricity, static magnetic eccentricity, and mixed magnetic eccentricity, which allows studying the phenomena of unbalance under the simultaneous action of forces of different nature.

Methodology

Mathematical model of rotor vibrations

In the proposed model, a rigid rotor of mass m of the motor has three degrees of freedom and, rotating with an angular velocity Ω , can make small translational movements in the direction of the x and z axes. In the model shown in Fig. 1, the following assumptions are made:

- the elastic characteristics of all supports are linear;
- the rotor is assumed to be rigid and its deformations are neglected;
- the position of the center of mass point S of the rotor is known;
- the stator is considered to be absolutely rigid and rigidly fixed to a rigid foundation.

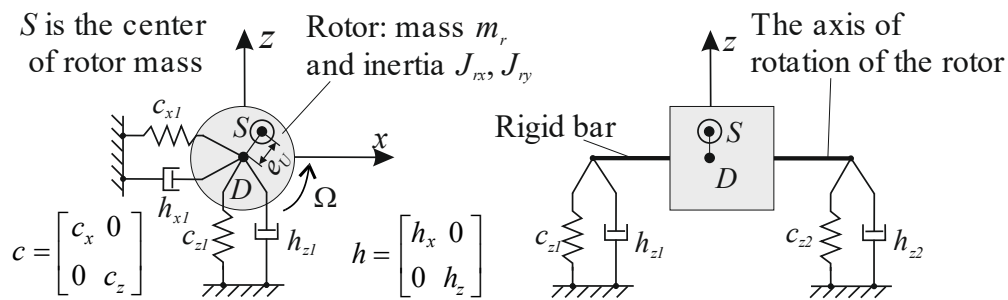


Fig. 1. Dynamic model of a rotor with mass eccentricity

In the diagram, the mass eccentricity is equal to $e_U = SD$, where point D is obtained as a result of the intersection of the rotor axis of rotation with a plane drawn through the center of mass point S perpendicular to the axis of rotation of the rotor. For generalized coordinates, we take the x, y coordinates of point D .

The kinetic energy of a system is defined as

$$T = \frac{1}{2} m \begin{pmatrix} \dot{x} & \dot{y} \end{pmatrix} \begin{pmatrix} \dot{x} \\ \dot{y} \end{pmatrix} \quad (1)$$

where \dot{x}_i, \dot{z}_i are projections of the full velocities of the point S ;

m is the mass of the rotor.

The center of mass point S performs a complex motion: translational with a velocity \dot{x}_i, \dot{z}_i and rotational with velocity Ω . Then the projections of the total velocities are defined as:

$$\dot{x}_i = \dot{x}_i + \Omega z_i, \quad \dot{z}_i = \dot{z}_i - \Omega x_i. \quad (2)$$

The potential energy of the system is determined through the elastic deformations of the bearing supports as

$$U = \frac{1}{2}(c_{x1} + c_{x2})x^2 + \frac{1}{2}(c_{z1} + c_{z2})z^2, \quad (3)$$

where $c_{x1}, c_{x2}, c_{z1}, c_{z2}$ are projections of the stiffness vectors of the supports 1 i 2.

The mechanical energy dissipation in the dampers of the supports is defined as

$$D = \frac{1}{2}(h_{x1} + h_{x2})\dot{x}^2 + \frac{1}{2}(h_{z1} + h_{z2})\dot{z}^2, \quad (4)$$

where $h_{x1}, h_{x2}, h_{z1}, h_{z2}$ are the projections of the viscous friction vectors of supports 1 and 2.

The differential equations of rotor oscillations are obtained from the Lagrange equation of the second kind, taking into account the energy dissipation during Rayleigh damping:

$$\frac{d}{dt} \left(\frac{\partial T}{\partial \dot{x}_i} \right) - \frac{\partial T}{\partial x_i} + \frac{\partial U}{\partial x_i} + \frac{\partial D}{\partial \dot{x}_i} = 0, \quad i = 1, 2. \quad (5)$$

Taking $\Omega = const$ in (5) we obtain a system of linear differential equations

$$\begin{aligned} m\ddot{x} + (c_{x1} + c_{x2})\dot{x} + (c_{x1} + c_{x2} - 2m\Omega^2)x &= \Omega^2 m e \sin \Omega t, \\ m\ddot{z} + (c_{z1} + c_{z2})\dot{z} + (c_{z1} + c_{z2} - 2m\Omega^2)z &= \Omega^2 m e \cos \Omega t. \end{aligned} \quad (6)$$

To analyze the effect of magnetic eccentricity, we use the approach described in [9, 10] (Fig. 2).

The value of the air gap of the eccentric rotor for an arbitrary eccentricity at any time is approximated:

$$\delta(\psi, t) \approx \delta_0 - e_m(t) \cos(\psi - \varphi(t)), \quad (7)$$

where δ_0 is the average value of air gap at rotor centering;

ψ is the stator position angle;

$e_m(t)$ is the value of magnetic eccentricity at time t ;

$\varphi(t)$ is position angle of eccentricity (rotation of the rotor center) at time t .

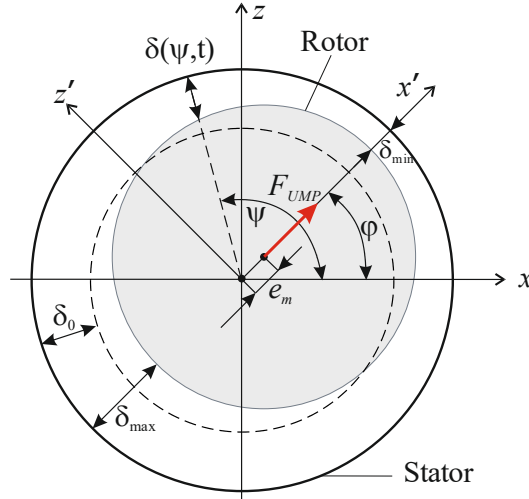


Fig. 2. Diagram of magnetic eccentricity of the rotor

At static eccentricity e_{ms} $\varphi = \text{const}$ is the position angle of static eccentricity. At dynamic eccentricity e_{md} the eccentricity position angle is a function of time $\varphi(t) = \varphi_0 + \Omega t$, where φ_0 is the initial position angle of the dynamic eccentricity.

UMP is highly nonlinear. The expression for the unbalanced magnetic pull on the rotor surface for number of pole pairs $p=1$ is defined as

$$\begin{aligned} F_{UMPx} &= f_1 \cos \varphi + f_2 \cos(2\omega t - \varphi) + f_3 \cos(2\omega t - 3\varphi), \\ F_{UMPz} &= f_1 \sin \varphi + f_2 \sin(2\omega t - \varphi) + f_3 \sin(2\omega t - 3\varphi), \end{aligned} \quad (8)$$

where F_{UMPx} and F_{UMPz} are projections of the magnetic pull force on the x and z axes, respectively;

ω is angular frequency of the motor stator winding power supply source;

f_1, f_2, f_3, f_4 are the amplitudes of the components of the UMP. They are calculated as follows,

$$\begin{aligned} f_1 &= 0.25Rl\pi\mu_0^{-1}F_j^2(2\Lambda_0\Lambda_1 + \Lambda_1\Lambda_2 + \Lambda_2\Lambda_3), \\ f_2 &= 0.125Rl\pi\mu_0^{-1}F_j^2(2\Lambda_0\Lambda_1 + \Lambda_1\Lambda_2 + \Lambda_2\Lambda_3), \\ f_3 &= 0.125Rl\pi\mu_0^{-1}F_j^2(2\Lambda_0\Lambda_3 + \Lambda_1\Lambda_2), \\ f_4 &= 0.125Rl\pi\mu_0^{-1}F_j^2\Lambda_2\Lambda_3, \end{aligned} \quad (9)$$

where R is the rotor radius;

l is the rotor length;

F_j is the amplitude of the fundamental wave of magnetomotive force (MMF) of rotor excitation;

μ_0 is the air permeance;

Λ_i are the Fourier coefficients in the expression of the magnetic permeability of the air gap, which can be calculated as

$$\Lambda_i = \frac{\mu_0}{\delta_0} \frac{1 + (1 - \delta_{i0})}{\sqrt{1 - \varepsilon^2}} \left(\frac{1}{1 + \sqrt{1 - \varepsilon^2}} \right)^i, \quad i \geq 0. \quad (10)$$

where $\varepsilon = \frac{e_m}{\delta_0}$ indicates relative eccentricity;

δ_{i0} is Kronecker symbol.

The angular speed of rotation of the rotor taking into account the slip s of the induction motor is related to the angular speed of rotation of the magnetic field ω_m and the angular frequency of the electric current supplying the winding ω as follows

$$\Omega = (1 - s)\omega_m = (1 - s)\frac{\omega}{p}, \quad (11)$$

where s is the slip of the induction motor.

Taking into account the mass eccentricity and UMP, we obtain a system of differential equations to describe the rotor behavior

$$\begin{aligned} m'' & \dots x = \Omega^2 m e \sin \Omega t + F_{UMPx}, \\ m'' & \dots z = \Omega^2 m e \cos \Omega t + F_{UMPz}. \end{aligned} \quad (12)$$

We will use numerical methods to solve this system of equations with a nonlinear right-hand side.

Simulation model for numerical calculation

The simulation model was created in the *Simulink/Simscape multibody* environment of the MATLAB mathematical package. The general view of the model is shown in Fig. 3. The simulation model contains the "Rigid rotor" block, which implements the mathematical model (6). The "Calc UMP" subsystem calculates UMP for static magnetic eccentricity, dynamic magnetic eccentricity, and mixed magnetic eccentricity according to Equations (8). The influence of magnetic pulling forces on the rotor is performed by the "External Force and Torque" block. The "Measuring unit" subsystem provides vibration measurement and analysis of the vibration spectrum.

A three-phase squirrel-cage induction motor with a power of 11 kW and an operating speed of 3000 rpm was chosen for the simulation. The motor parameters are shown in Table 1.

Table 1. Parameters of the three-phase induction motor

Notation	Description	Value
Motor data		
n	Rated speed (rpm)	3000
s	Rated slip	0.033
R	Radius of the rotor (mm)	63.5
l	Length of the rotor (mm)	130
m_r	Mass of the rotor (kg)	14.22
m_s	Mass of the stator (kg)	57.78
δ_0	Mean air-gap length (mm)	0.45
μ_0	Air permeance (H/m)	$4\pi \cdot 10^{-7}$
F_j	Fundamental MMF amplitude of the rotor excitation current (A)	945
p	Number of pole pairs	1
c_{rx}, c_{rz}	Stiffness of bearing housing and end shield (N/m)	$5.52 \cdot 10^7$

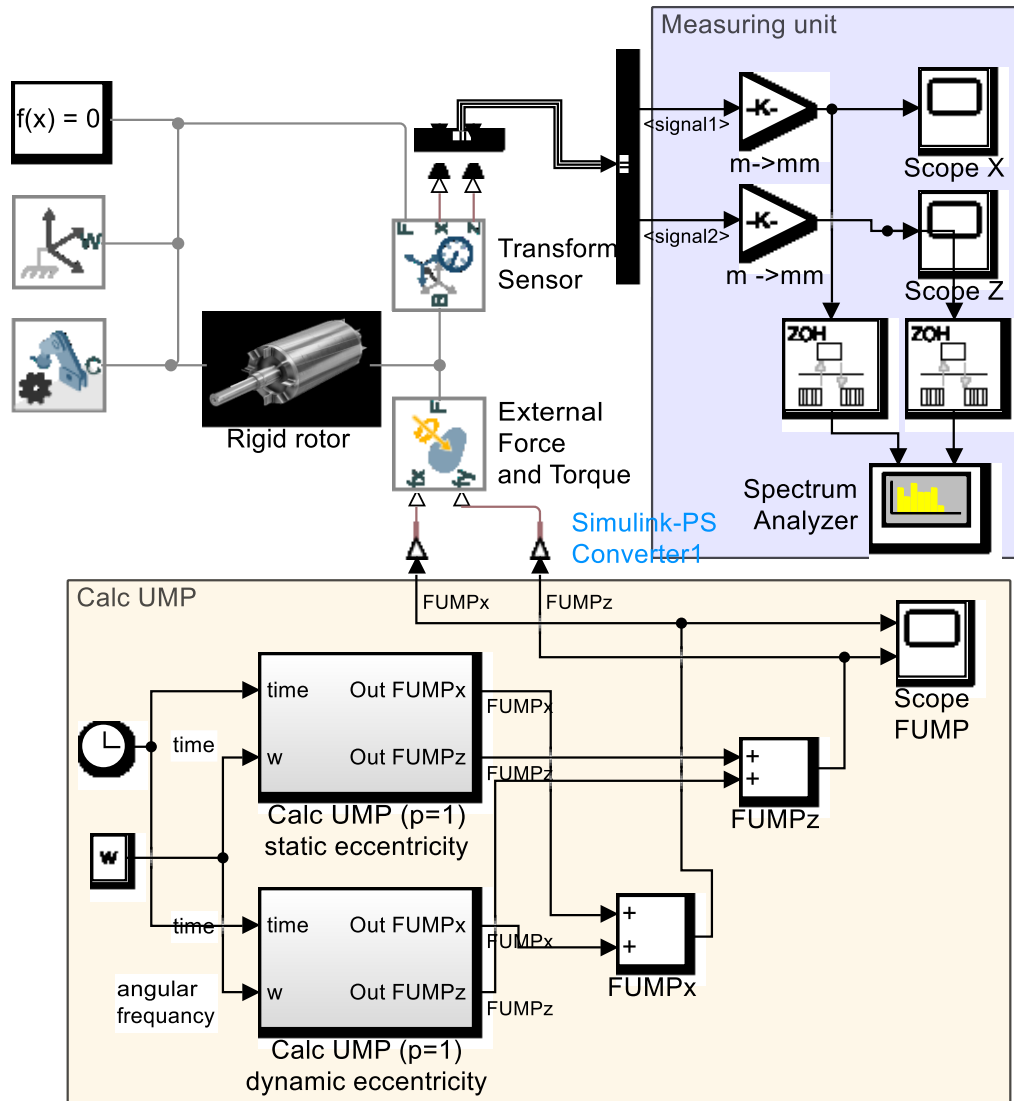


Fig. 3. Simulation model of rotor research

Simulation Results and Discussion

The simulation of the vibration process according to (12) was carried out at an operating rotor speed of $n=2910$ rpm, which corresponds to an angular rotation frequency of $\Omega=303.5$ rad/s. The images of the rotor vibration signals along the z-axis at the value of the relative static magnetic eccentricity $\varepsilon=5\%$ are shown in Figs. 4-6. The image of the vibration signal spectrum at mixed magnetic eccentricity is shown in Fig. 7.

The static magnetic eccentricity causes a vibration with a double frequency 2ω of the electric one. In the spectrogram (Fig. 7), this harmonic is observed at a frequency of $f=93.75$ Hz. In addition, the static magnetic eccentricity causes the rotor to shift in the direction of the minimum air gap, which corresponds to the zero harmonic $f=0$.

Under the influence of dynamic eccentricity, the entire spectrum is centered on the rotor speed $f=48.8$ Hz. The time vibration signal is modulated with the rotor precession frequency.

Mixed magnetic eccentricity, which is most common in practice, is a source of a complex non-sinusoidal signal.

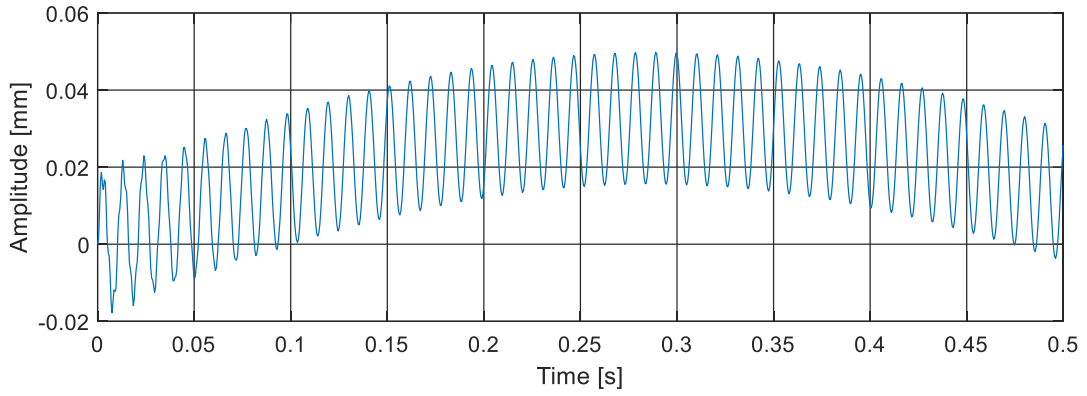


Fig. 4. Vertical rotor vibrations with static magnetic eccentricity $\varepsilon=5\%$

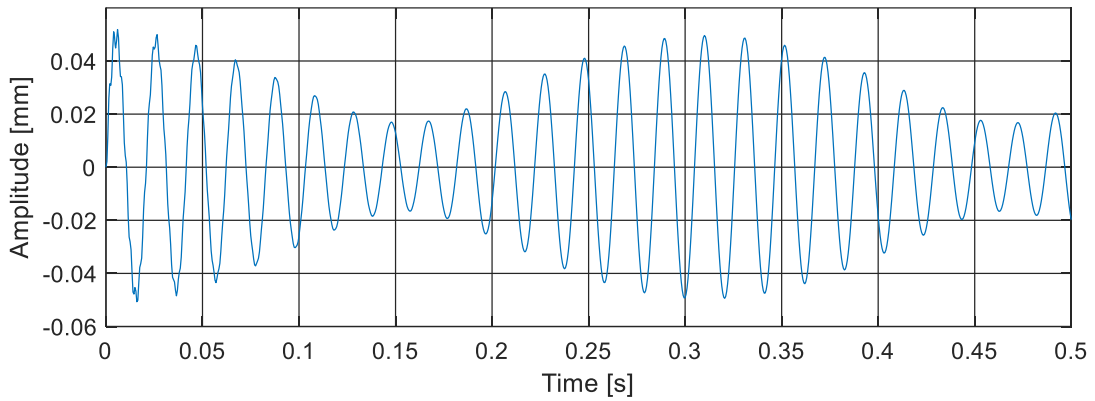


Fig. 5. Vertical rotor vibrations with dynamic magnetic eccentricity $\varepsilon=5\%$

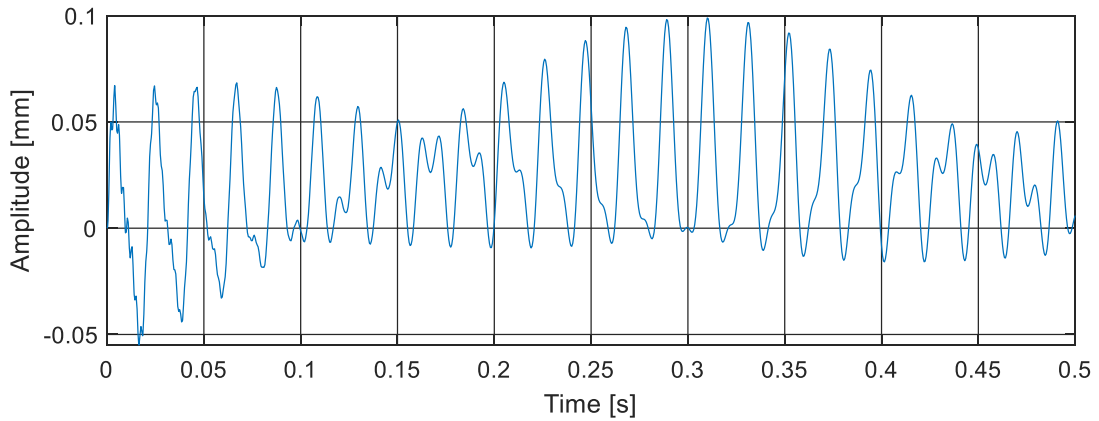


Fig. 6. Vertical vibrations of a rotor with mixed magnetic eccentricity $\varepsilon=5\%$

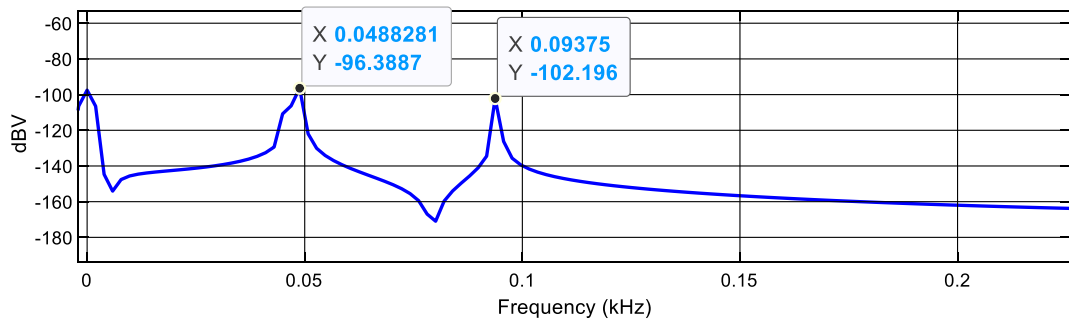


Fig. 7. Vibration signal spectrum at mixed magnetic eccentricity

Conclusion

The work created a mathematical model of oscillations of a rigid rotor, which oscillates on two elastic supports, taking into account mass and magnetic eccentricity.

Vibrations caused by static magnetic eccentricity occur at twice the electrical frequency. This feature reduces the overall rigidity of the rotor and lowers the critical rotor frequencies, which must be significantly higher than the operating frequency.

Vibrations caused by dynamic eccentricity take the form of a rotor speed signal modulated at a low frequency depending on the rotor precession.

The model can be used for vibration diagnostics of electric motor rotor eccentricity.

Bibliography

1. Popa, L. M., Jensen, B. B., Ritchie, E., et al. (2003). Condition monitoring of wind generators. 38th IAS Annual Meeting on Conf. Record of the Industry Applications Conf., Salt Lake City, Utah, USA, vol. 3, pp. 1839 - 1846
2. Salah, A. A., Dorrell, D. G., Guo, Y. (2019). A Review of the Monitoring and Damping Unbalanced Magnetic Pull in Induction Machines Due to Rotor Eccentricity. In IEEE Transactions on Industry Applications. 55(3). pp. 2569-2580
3. Normanyo, E., Prince Nkansah, J. (2021). Damping of Unbalanced Voltage-Caused Vibrations of Induction Motors. International Journal of Mechatronics, Electrical and Computer Technology (IJMEC). 11(42), pp. 5065-5073
4. Zhu, Rui, et al. (2023). Calculation and Analysis of Unbalanced Magnetic Pull of Rotor under Motor Air Gap Eccentricity Fault. Sustainability, 15(11), pp. 8537.
5. Kim, H., Sikanen, E., Nerg, J., Sillanpää, T., & Sopanen, J. T. (2020). Unbalanced magnetic pull effects on rotordynamics of a high-speed induction generator supported by active magnetic bearings—analysis and experimental verification. IEEE Access, 8, 212361-212370.
6. Werner, U. (2017). Mathematical multibody model of a soft mounted induction motor regarding forced vibrations due to dynamic rotor eccentricities considering electromagnetic field damping. Journal of Applied Mathematics and Physics, 5(2). 346-364.
7. Dorrell, D. G., & Salah, A. (2015). Detection of rotor eccentricity in wound rotor induction machines using pole-specific search coils. IEEE Transactions on Magnetics, 51(11), 1-4.
8. Mazur, D., & Trojnar, M. (2003). Modelling of electrical and mechanical phenomena in induction motors with air-gap eccentricity. In Proc. International Conference on Renewable Energy and Power Quality ICREPQ (p. 2003).
9. Du, J., & Li, Y. (2023). Analysis on the variation laws of electromagnetic force wave and vibration response of squirrel-cage induction motor under rotor eccentricity. Electronics, 12(6), 1295.
10. Wang, Z., He, W., Du, S., Yuan, Zh. (2021). Study on the Unbalanced Fault Dynamic Characteristics of Eccentric Motorized Spindle considering the Effect of Magnetic Pull. Shock and Vibration, vol. 2021, pp. 1-12